

A Novel Family of Phosphole-Thiophene Oligomers for Optoelectronic Applications

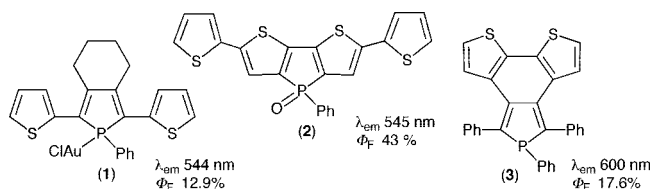
Ngoc Hoa Tran Huy,^{*,†} Bruno Donnadiou,[†] François Mathey,^{*,†} Astrid Muller,[‡] Kathryn Colby,[‡] and Christopher J. Bardeen[‡]

UCR-CNRS Joint Research Chemistry Laboratory, Department of Chemistry, University of California Riverside, Riverside, California 92521-0403

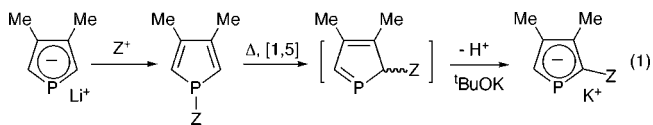
Received July 8, 2008

A 2-terthienylphospholide can be prepared from a 1-terthienylphosphole by reaction with *t*BuOK in diglyme at 150 °C. This phospholide is then transformed into the corresponding 1-methyl-2-terthienylphosphole-borane. This borane complex fluoresces at 510 nm in CH₂Cl₂ with a quantum yield of 0.17. The excited-state displays a significant charge transfer between the terthienyl substituent and the phosphole ring as shown by the shift of the emission to lower energies upon increasing the polarity of the solvent.

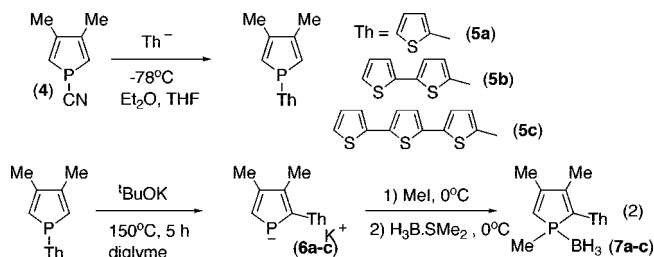
Three groups have definitively established the fact that conjugated thiophene-phosphole oligomers display an impressive potential for the manufacture of organic light emitting diodes (OLEDs). A typical product developed by the group of Réau is phosphole gold complex (1).¹ Dithienophosphole (2) is representative of the work of Baumgartner.^{2a} Matano has recently developed another type of thieno-annellated phosphole represented by 3.^{2b} Other related systems have also been described.³



Some time ago, we developed a simple and efficient method to functionalize the phosphole ring on the α -position (eq 1).⁴ We



decided to apply this method to the preparation of a novel family of thiophene-phosphole oligomers for optoelectronic applications. Our starting point was the 1-cyano derivative (4).⁵ The chemistry is depicted in eq 2. By comparison with the classical procedure as devised for the [1,5] migration of the phenyl group,⁴ the main change is the use of diglyme as the solvent



for the reaction at high temperature. The use of THF leads to impure phospholide ions. These ions were only characterized by ³¹P NMR spectroscopy— $\delta^{31}\text{P}$ 74.9 (6a), 79.7 (6b), and 81.6 (6c)—and were used as such for further transformation. The final products (7a-c) were characterized by mass spectrometry and NMR spectroscopy. Compound 7b was also characterized by X-ray crystal structure analysis (Figure 1). The most characteristic features of the structure are the perfect coplanarity of the three rings, the high dis-symmetry of the phosphole ring (P1–C1 1.762(3) vs P1–C4 1.810(3) Å) and the short bridge bonds between the rings (C4–C5 1.443(4) and C8–C9 1.452(4) Å). The packing of the molecules in the crystal is shown in (Figure 1a). The distance between the planes is ca. 4 Å.

The planarity and short bond lengths would be expected to support significant electronic delocalization between the three rings. Indeed, when compared to the analogous thiophene compounds, we find similar spectroscopic behavior. Table 1 summarizes the quantum yield and lifetime measurements for compounds 7b and 7c as well as those of terthiophene and quaterthiophene. Note that our independently measured values for terthiophene agree well with literature values.⁶ The phosphole analogs undergo about a 30 nm redshift in peak absorption and fluorescence wavelengths with the addition of an extra thiophene ring, as compared to about a 40 nm shift in the oligothiophenes. The fluorescence quantum yield and lifetime of the phosphole derivative 7b is comparable to its thiophene analog, whereas the lifetime of 7c is considerably longer than that of quaterthiophene. These spectroscopic measurements were performed in dilute solutions with concentrations of 10⁻⁵ M or

* E-mail: fmathey@citrus.ucr.edu.

[†] UCR-CNRS Joint Research Chemistry Laboratory.

[‡] Department of Chemistry.

(1) Su, H.-C.; Fahdel, O.; Yang, C.-J.; Cho, T.-Y.; Fave, C.; Hissler, M.; Wu, C.-C.; Réau, R. *J. Am. Chem. Soc.* **2006**, *128*, 983.

(2) (a) Dienes, Y.; Durben, S.; Kárpáti, T.; Neumann, T.; Englert, U.; Nyulaszi, L.; Baumgartner, T. *Chem.—Eur. J.* **2007**, *13*, 7487. (b) Miyajima, T.; Matano, Y.; Imahori, H. *Eur. J. Org. Chem.* **2008**, 255.

(3) (a) Na, H.-S.; Morisaki, Y.; Aiki, Y.; Chujo, Y. *J. Polym. Sci., Part A* **2007**, *45*, 2867. Sanji, T.; Shiraiishi, K.; Kashiwabara, T.; Tanaka, M. *Org. Lett.* **2008**, *10*, 2689.

(4) Holand, S.; Jeanjean, M.; Mathey, F. *Angew. Chem., Int. Ed. Engl.* **1997**, *36*, 98. (b) Mathey, F. *Acc. Chem. Res.* **2004**, *37*, 954.

(5) Holand, S.; Mathey, F. *Organometallics* **1988**, *7*, 1796.

(6) Becker, R. S.; de Melo, J. S.; Macanita, A. L.; Elisei, F. *J. Phys. Chem.* **1996**, *100*, 18683.

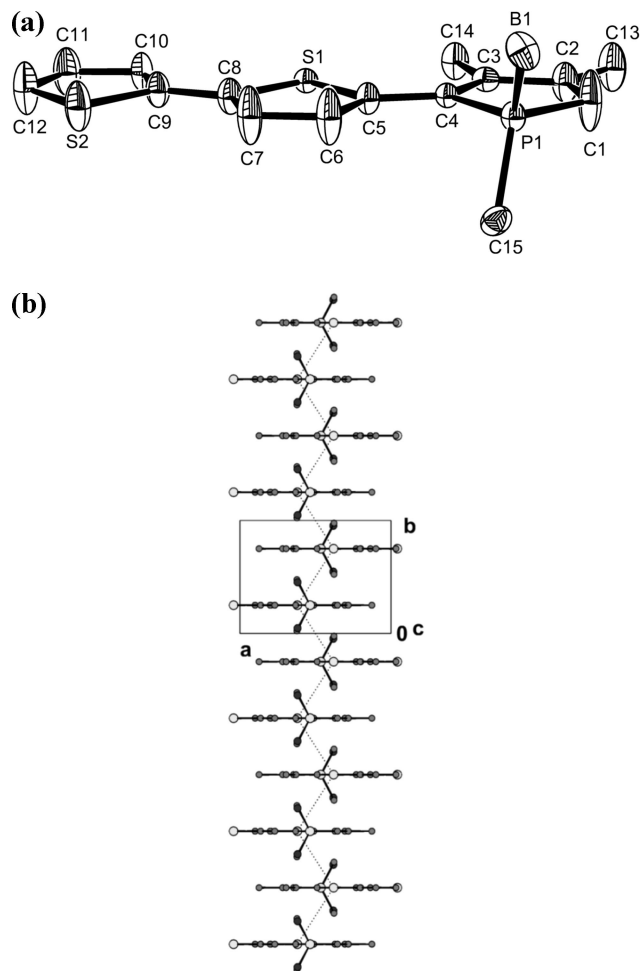


Figure 1. Panel a: X-ray crystal structure analysis of (**7b**). Significant distances (Å) and angles (°): P1–B1, 1.865(9); P1–C1, 1.762(3); P1–C4, 1.810(3); P1–C15, 1.861(8); C1–C2, 1.338(5); C2–C3, 1.478(4); C3–C4, 1.366(4); C4–C5, 1.443(4); C5–S1, 1.736(3); C5–C6, 1.384(4); C6–C7, 1.398(5); C7–C8, 1.368(4); S1–C8, 1.725(3); C8–C9, 1.452(4); C9–S2, 1.719(3); S2–C12, 1.708(4); C12–C11, 1.353(5); C11–C10, 1.432(5); C10–C9, 1.414(5); C1–P1–C4, 92.34(15); P1–C4–C5, 120.35(19); C4–C5–S1, 124.5(2); C5–S1–C8, 92.84(14); S1–C8–C9, 121.1(2); C8–C9–S2, 119.7(2); C9–S2–C12, 91.86(17). Panel b: Crystal packing of (**7b**).

Table 1. Spectroscopic Parameters for Oligothiophenes and Phosphole Analogs Made in This Work^a

	λ_{abs} (nm)	λ_{fl} (nm)	τ_{fl} (ns)	Φ_{fl}	τ_{rad} (ns)	$\Delta\mu$ (debye)
7b	384.3, 382.6	469.5, 476.4	0.100	0.016	6.3	3.8
7c	410.7, 409.1	502.0, 511.0	1.22	0.178	6.9	4.4
terthiophene	354.5, 354.3	421.6, 420.5	0.188	0.060	3.1	0.4
quaterthiophene	392	478	0.49	0.18	2.7	

^a For the peak absorption and fluorescence wavelengths λ_{abs} and λ_{fl} , the first value is in toluene and second is in CH_2Cl_2 . For quaterthiophene, data are taken in dioxane from ref 6.

less, where concentration-dependent effects such as aggregation could not be observed. Such effects would be expected to be important in the solid-state spectroscopy of these compounds and would determine their performance in devices such as OLEDs. Solid-state spectroscopic studies are beyond the scope of the current work but are the subject of future planned studies.

An important difference between the thiophene and phosphole compounds is the fact that the absorption and emission are shifted to longer wavelengths in the phosphole compounds. For

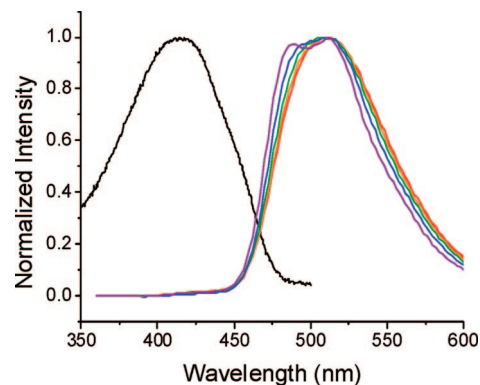


Figure 2. Black: **7c** absorption in 100% toluene. The absorption in 100% CH_2Cl_2 is the same. Purple: fluorescence in 100% toluene; blue: fluorescence in 75% toluene and 25% CH_2Cl_2 ; green: fluorescence in 50% toluene and 50% CH_2Cl_2 ; orange: fluorescence in 25% toluene and 75% CH_2Cl_2 ; red: fluorescence in 100% CH_2Cl_2 . Note that terthiophene shows at most a 1 nm shift under the same conditions.

example, changing a thiophene to a phosphole shifts the peak absorption from 354 nm in terthiophene to 384 nm in **7b**. The shifts in wavelength suggest that the excited states in **7b** and **7c** have different electronic characteristics from those of pure oligothiophenes. Closer inspection of the fluorescence lifetime data also suggests different excited-state characteristics for the phospholes. The length dependence of the phosphole fluorescence lifetimes is much more pronounced in the phospholes than in the thiophenes, increasing by a factor of 10 from **7b** to **7c** as opposed to less than a factor of 3 from terthiophene to quaterthiophene. The fluorescence lifetime contains contributions from both radiative and nonradiative processes, and the former appear to be more effectively suppressed in the longer phospholes. The radiative lifetime τ_{rad} is given by

$$\tau_{\text{rad}} = \frac{\tau_{\text{fl}}}{\Phi_{\text{fl}}}$$

and is determined by the intrinsic oscillator strength of the excited state. Table 1 shows that **7b** and **7c** have radiative lifetimes of 6–7 ns, whereas those of the thiophenes are 2.7–3.1 ns, at least a factor of 2 smaller. This indicates that the fluorescence oscillator strength in the phospholes is significantly weaker than in the thiophenes.

To further probe the nature of the excited states, we varied the polarity of the solvent. Excited states with more charge transfer character should show fluorescence spectra that shift to lower energies in more polar solvents. That is exactly what we see in the phosphole analog **7c** (Figure 2). Using a blend of CH_2Cl_2 and toluene, we could vary the solvent polarity continuously and observe a continuous shift in the fluorescence.⁷ By plotting the fluorescence Stokes shift versus solvent polarity, we obtain the linear plots shown in Figure 3. From these plots, using the Lippert–Mataga formula, we can extract the change in dipole moment upon photon absorption ($\Delta\mu$), which gives an indication of the charge transfer nature of the excited state (more charge transfer leads to larger change in dipole moment or larger value for $\Delta\mu$).^{7–9} For terthiophene, the change in dipole is only 0.6 debye, whereas for **7b** and **7c** the changes are 3.8

(7) Hirata, Y.; Mataga, N. *J. Phys. Chem.* **1984**, *88*, 3091.

(8) Edward, J. J. *Chem. Educ.* **1970**, *47*, 261.

(9) Thompson, A. L.; Ahn, T.; Thomas, K. R. J.; Thayumanavan, S.; Martinez, T. J.; Bardeen, C. J. *J. Am. Chem. Soc.* **2005**, *127*, 16348.

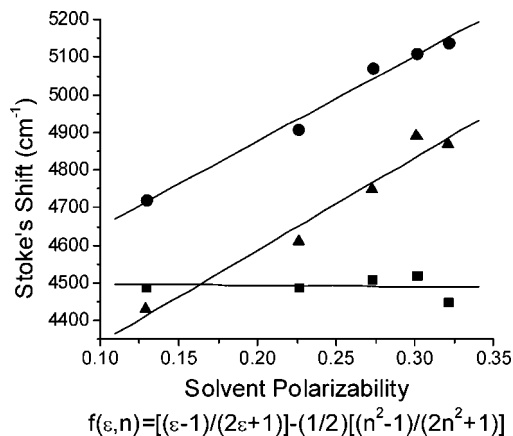


Figure 3. Plots of Stokes shift (Δ_{SS}) versus solvent polarity parameter for **7b** (●), **7c** (▲), and terthiophene (■). The Lippert–Mataga equation then allows the extraction of the dipole moment change $\Delta\mu$ from the relation $\Delta_{SS} = (2\Delta\mu^2)/(hca^3)f(\epsilon,n)$ where h is Planck's constant, c is the speed of light, and a is the molecular radius, obtained from the relation molecular volume = $(4/3)\pi a^3$.

and 4.4 debye, respectively, with about 10% error in all values. The larger values for $\Delta\mu$ confirm that the phosphole analogs have excited states with greater charge transfer character than the oligothiophenes, and this may help explain their different spectroscopic properties. Chemically modulating this transfer would be interesting. The synthetic route that we have used allows such a modulation. We can replace the terthiophene by a longer oligothiophene, change the substitution at phosphorus and graft a functional substituent at the α' position of the phosphole ring using the chemistry depicted in eq 1.

Experimental Section

Nuclear magnetic resonance spectra were obtained on a Bruker Avance 300 and Varian Inova spectrometers operating at 300.13 MHz for ^1H , 75.45 MHz for ^{13}C , and 121.496 MHz for ^{31}P . Chemical shifts are expressed in parts per million (ppm) downfield from external TMS (^1H and ^{13}C) and external 85% H_3PO_4 (^{31}P). Mass spectra were obtained on VG 7070 and Hewlett–Packard 5989A GC/MS spectrometers. Elemental analyses were performed by Desert Analytics Laboratory, Tucson, Az. The synthesis of **5b** is described in ref 10.

1-(2-Thienyl)-3,4-Dimethyl Phosphole (5a). To a solution of thiophene (1 mL, 12 mmol) in Et_2O (30 mL), BuLi (8.5 mL of 1.5 M in hexanes) was added dropwise at 0 °C. The mixture was stirred for 1 h at room temperature, cooled at -78 °C, and then a solution of cyanophosphole (**4**) (14 mmol in 25 mL of THF) was added. After stirring for 0.5 h at -78 °C and for 1 h at room temperature, the solution was evaporated under vacuum, and the crude product was chromatographed on silica gel with hexane/dichloromethane 9:1 as the eluent. Compound **5a** was recovered as white crystals in 62% yield (1.2 g). ^{31}P NMR (CH_2Cl_2): δ -22.4 ppm. The product has already been described.¹¹

[2-(2-Thienyl)-1,3,4-trimethylphosphole]borane (7a). A solution of phosphole (**5a**) (0.2 g, 1 mmol), *t*BuOK (0.08 g) in diglyme (2 mL) was heated in a pressure tube at 150 °C for 5 h. The formation of the phospholide anion (**6a**) was monitored by ^{31}P NMR: δ = 74.9 (diglyme). A solution of MeI (0.05 mL) in THF (0.8 mL) was added at 0 °C to this solution, which was further

stirred at room temperature for 0.5 h. The ^{31}P NMR showed a signal at δ -12.3 ppm. A solution of $\text{BH}_3 \cdot \text{SMe}_2$ (2M, 0.4 mL) was finally added to the reaction mixture at 0 °C. After being stirred for 0.5 h, the solvent was evaporated under vacuum, and the product was purified by chromatography on silica gel with hexane/dichloromethane 3:2 as the eluent; 0.12 g of light yellow crystals were obtained (55% yield). ^{31}P NMR (CDCl_3): δ 33.7. ^1H NMR (CDCl_3): δ 1.43 (d, $^2J_{\text{HP}}$ = 10.9 Hz, 3H, P–Me), 2.13 (d, $^4J_{\text{HP}}$ = 1.56 Hz, 3H, Me), 2.25 (s, 3H, Me); 6.14 (d, $^2J_{\text{HP}}$ = 33.6 Hz, 1H, =CHP), 7.09 (t, Th H₄), 7.37 (d, Th H_{3 or 5}), 7.40 (d, Th H_{5 or 3}). ^{13}C NMR (CDCl_3): δ 9.62 (d, $^1J_{\text{CP}}$ = 35.3 Hz, P–Me), 15.69 (d, $^3J_{\text{CP}}$ = 9.20 Hz, Me), 19.11 (d, $^3J_{\text{CP}}$ = 12.3 Hz, Me), 120.78 (d, $^1J_{\text{CP}}$ = 55.2 Hz, =CHP); 126.61, 127.77, 128.19 (Th CH); 145.25 (d, $^2J_{\text{CP}}$ = 15.34 Hz, =C–Me); 156.28 (d, $^2J_{\text{CP}}$ = 7.67 Hz, =C–Me). Mass: m/z 209 (M-BH_2^+ , 100%).

[2-(2-Bithienyl)-1,3,4-trimethylphosphole]borane (7b). Same procedure as for **7a**. The phosphole–borane complex (**7b**) was isolated as orange crystals (0.15 g, 50% yield). ^{31}P NMR (CDCl_3): δ 33.90. ^1H NMR (CDCl_3): δ 1.46 (d, $^2J_{\text{HP}}$ = 10.7 Hz, 3H, P–Me), 2.14 (d, $^4J_{\text{HP}}$ = 1.56 Hz, 3H, Me), 2.29 (s, 3H, Me), 6.15 (d, $^2J_{\text{HP}}$ = 35.45 Hz, 1H, =CHP), 7.09, 7.39 (m, 5H, Th H). ^{13}C NMR (CDCl_3): δ 9.85 (d, $^1J_{\text{CP}}$ = 35.3 Hz, P–Me), 15.85 (d, $^3J_{\text{CP}}$ = 7.7 Hz, Me), 19.12 (d, $^3J_{\text{CP}}$ = 12.3 Hz, Me), 120.76 (d, $^1J_{\text{CP}}$ = 55.2 Hz, =CHP); 124.26, 124.31, 125.16; 128.18; 129.20 (Th CH); 144.80 (d, $^2J_{\text{CP}}$ = 15.34 Hz, =C–Me); 156.38 (d, $^2J_{\text{CP}}$ = 7.67 Hz, =C–Me). Mass: m/z 291.04 (M-BH_2^+ , 100%). Anal. Calcd for $\text{C}_{15}\text{H}_{18}\text{BPS}_3$: C, 59.22; H, 5.96. Found: C, 58.92; H, 5.92. X-ray single crystals were obtained by slow recrystallization in a mixture of hexane and dichloromethane.

1-(2-Terthienyl)-3,4-dimethyl Phosphole (5c). Phosphole (**5c**) was prepared as indicated for the synthesis of **5a** from terthiophene (1.70 g, 7 mmol) in Et_2O (80 mL) and cyanophosphole (1.15 g, 8.4 mmol) in THF (20 mL). It was obtained in 40% yield (1.0 g) as yellow crystals. ^{31}P NMR (CDCl_3): δ -22.8 . ^1H NMR (CDCl_3): δ 2.12 (d, $^4J_{\text{HP}}$ = 2.35 Hz, 6H, Me), 6.42 (d, $^2J_{\text{HP}}$ = 39.0 Hz, 2H, =CHP), 7.09, 7.25 (m, 7H, Th H). ^{13}C NMR (CDCl_3): δ 17.89 (s, Me), 149.93 (d, $^2J_{\text{CP}}$ = 7.77 Hz, =C–Me). Mass: m/z 359 (MH^+ , 100%). Anal. Calcd for $\text{C}_{18}\text{H}_{15}\text{PS}_3$: C, 60.31; H, 4.22. Found: C, 60.45; H, 4.50.

[2-(Terthienyl)-1,3,4-trimethylphosphole]borane (7c). Using the same procedure as described above for the synthesis of **7a** from **5c** (0.36 g, 1 mmol). The phosphole–borane complex was isolated as orange crystals (0.2 g, 50% yield). ^{31}P NMR (CDCl_3): δ 33.8. ^1H NMR (CDCl_3): δ 1.47 (d, $^2J_{\text{HP}}$ = 10.9 Hz, 3H, P–Me), 2.15 (d, $^4J_{\text{HP}}$ = 1.57 Hz, 3H, Me), 2.30 (s, 3H, Me), 6.16 (d, $^2J_{\text{HP}}$ = 34.35 Hz, 1H, =CHP), 7.09, 7.39 (m, 7H, Th H). ^{13}C NMR (CDCl_3): δ 9.90 (d, $^1J_{\text{CP}}$ = 35.3 Hz, P–Me), 15.87 (d, $^3J_{\text{CP}}$ = 9.2 Hz, Me), 19.12 (d, $^3J_{\text{CP}}$ = 12.3 Hz, Me), 120.81 (d, $^1J_{\text{CP}}$ = 55.2 Hz, =CHP), 124.26, 124.31, 125.16, 128.18, 129.20 (Th CH), 144.93 (d, $^2J_{\text{CP}}$ = 15.33 Hz, =C–Me), 156.39 (d, $^2J_{\text{CP}}$ = 6.14 Hz, =C–Me). Mass: m/z 373 (M-BH_2^+ , 100%). Anal. Calcd for $\text{C}_{19}\text{H}_{20}\text{BPS}_3$: C, 59.07; H, 5.22. Found: C, 59.16; H, 5.13.

Crystal Structure Determination of (7b). Measurements were carried out using a low-temperature device at $T = 100(2)$ K on a BRUKER X8-APEX¹² KAPPA-CCD X-Ray diffractometer system (Mo-radiation, $\lambda = 0.71073$ Å). An automated strategy determination program COSMO¹³ was used to define diffraction experiments on the basis of phi and omega scans. Frames were integrated using the Bruker SAINT version 7.06A software¹⁴ and using a narrow-frame integration algorithm. The integrated frames yielded a total of 8828 reflections collected at a maximum 2θ angle of 57.56° (2075 independent reflections, $R_{\text{int}} = 0.0342$, $R_{\text{sig}} = 0.0278$, completeness = 99.7%), and 1802 (86.84%) reflections were found

(10) Bevierre, M. O.; Mercier, F.; Ricard, L.; Mathey, F. *Angew. Chem., Int. Ed. Engl.* **1990**, *29*, 655.

(11) Bevierre, M. O.; Mercier, F.; Ricard, L.; Mathey, F. *Bull. Soc. Chim. Fr.* **1992**, *129*, 1.

(12) APEX 2, v. 2.0–2; Bruker AXS Inc.: Madison, Wisconsin, 2004.

(13) COSMO NT, v. 1.40; Bruker AXS Inc.: Madison, Wisconsin, 2004.

(14) SAINTPLUS Software Reference Manual, v. 6.02A; Bruker Analytical X-Ray System, Inc.: Madison, WI, 1997–1998.

greater than $2\sigma(I)$. Compound crystallizes in monoclinic cell, space group $P2(1)/m$, $a = 9.5684(3)$ Å, $b = 7.1449(3)$ Å, $c = 11.3682(4)$ Å, $\alpha = 90.0^\circ$, $\beta = 91.944(2)^\circ$, $\gamma = 90.0^\circ$, $V = 776.74(5)$ Å³, $Z = 2$, calculated density $D_c = 1.339$ Mg/m³. Absorption corrections were applied for all data using the SADABS program included in the SAINTPLUS software package.¹⁴ Direct methods using the Sir92 program¹⁵ was used for resolution. Direct methods of phase determination followed by some subsequent difference Fourier map led to an electron density map from which most of the non-hydrogen atoms were identified in the asymmetry unit. With subsequent isotropic refinement and some Fourier differences synthesis, all non-hydrogen atoms were identified, and atomic coordinates and isotropic and anisotropic displacement parameters of all the non-hydrogen atoms were refined by means of a full matrix least-squares procedure on F^2 , using SHELXTL software.¹⁶ Hydrogen atoms were included in the refinement in calculated positions with isotropic thermal parameters fixed at 20 and 50% higher than Csp^2 and Csp^3 atoms, respectively, to which they were connected; torsion angles were refined for methyl groups. The refinement converged at $R1 = 0.0553$, $wR2 = 0.1463$, with intensity $I > 2\sigma(I)$, and the largest peak/hole in the final difference map were found at 0.669 and -0.581 e \cdot Å⁻³. Drawing of the molecule was achieved using ORTEP32.¹⁷ Further details on the crystal structure investigation are available on request from the Director of the Cambridge Crystallographic Data center, 12 Union Road, GB-Cambridge CB21EZ UK, on quoting the full journal citation.

(15) Altomare, A.; Cascarano, G.; Giacovazzo, C.; Guagliardi, A. *J. Appl. Crystallogr.* **1993**, *26*, 343.

(16) *SHELXTL Software Reference Manual*, v. 6.10, Dec. 5th, 2000; Bruker Analytical X-Ray System, Inc.: Madison, WI., 2000.

(17) Farrugia, L. J. *J. Appl. Crystallogr.* **1997**, *30*, 565.

Spectroscopic Measurements. Samples were prepared with peak absorbances ≤ 0.2 to avoid self-absorption artifacts. Absorption spectra were taken on a Cary50Bio. Fluorescence spectra were taken on a Horiba Jobin Yvon-Spex Fluorolog-3 Fluorimeter with excitation at 350 nm and were integrated from 360–660 nm with manual solvent subtraction. All spectra were measured in a 1 cm fused silica quartz cuvette. Solvent polarity was varied by mixing CH₂Cl₂ and toluene to get 100:0, 75:25, 50:50, 25:75, and 0:100 CH₂Cl₂/toluene mixtures. The values of ϵ and n for these solvent mixtures were calculated⁷ and were used to find the respective mixtures' solvent polarizabilities. The molecular volumes were calculated⁸ and were used with the slope of the Lippert–Mataga plots to find the changes in the dipole moments between the excited and ground states.⁹ Fluorescence lifetime measurements were performed in dilute CH₂Cl₂ solutions using a 40 kHz repetition rate laser with 150 fs pulses centered at 400 nm for excitation and a Hamamatsu C4334 Streakscope to detect the fluorescence.

Supporting Information Available: X-ray crystal structure analysis of compound **7b** and NMR spectra of **7a** and **7b** are separately provided. This material is available free of charge via the Internet at <http://pubs.acs.org>.

Acknowledgment. This work has been partly supported by the University of California Riverside and the CNRS. F.M. acknowledges the Donors of the American Chemical Society Petroleum Research Fund for support of this research (ACS-PRF grant No. 44734-AC1). C.J.B. acknowledges the support of the National Science Foundation, grant No. CHE-0719039.

OM800644M